Journal of Directed Energy, **4**, Fall 2010, 71–97

Fabrication and Processing Technologies for Thin-Disk Laser Elements

Nicholas G. Traggis*, Neil R. Claussen, Christopher S. Wood, and Ove Lyngnes

Precision Photonics Corporation, Boulder, Colorado 80301

With the continued advancement of high power, solid-state laser technology, a thorough understanding of optical fabrication techniques and how they impact spectral performance, thermal management, and damage threshold is required. Given their very unique form factor, thin disk lasers offer particular challenges in fabrication. This paper presents a review of fabrication technologies for thin-disk laser elements. In particular, we review current technologies for polishing, assembly, thin film coating, mounting, and metrology.

KEYWORDS: CADB®, Epoxy-free, Adhesive-free YAG, Ion beam sputtering, Laser damage threshold, Soldering, Thin disk, Solid-state laser

1. Introduction

While providing excellent performance benefits, the fabrication of thin disk elements offers many unique challenges. The aspect ratio of the gain medium presents difficulties in achieving the polishing requirements for flatness and parallelism needed to maintain the beam quality that the devices are known for. At the same time, mounting and assembly methods must consider both thermal dissipation and distortion of the device at elevated temperatures. And finally, optical coatings must be of sufficiently low loss and high damage threshold to survive the typical power/fluence levels seen in the current state of the art.

In this paper, we review the current processing technologies utilized to overcome these challenges. We begin with the polishing methods and metrology techniques needed to meet reflected and transmitted wavefront requirements for both ceramic and single crystal materials. We then give a review of the current, high energy coating processes used to deposit optical thin films on these devices as well as a review of current assembly methodologies utilized to minimize loss and improve thermal properties. For reference, we will be assuming a standard capped thin disk element in most of these discussions, as shown in Fig. 1.

*Corresponding author; e-mail: ntraggis@precisionphotonics.com.

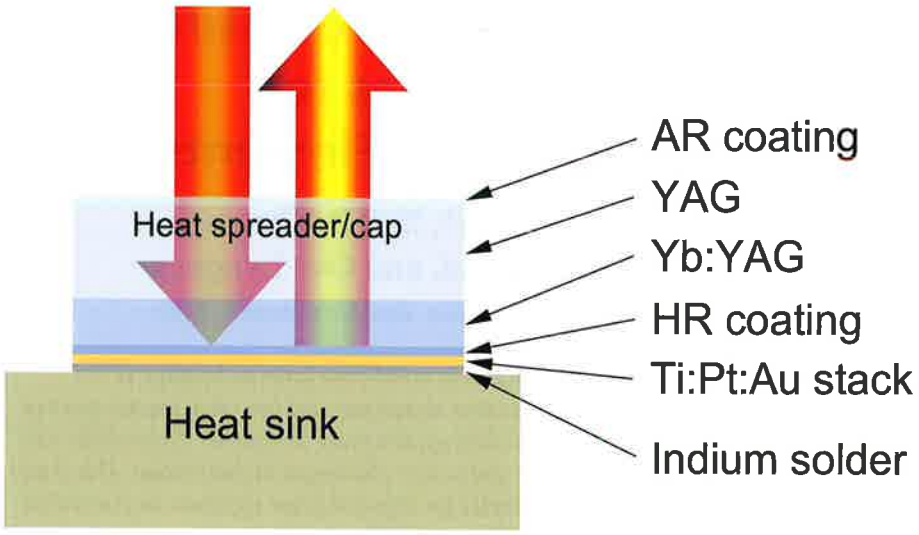

Fig. 1. Typical capped thin-disk element configuration.

2. Polishing

One of the most important aspects of disk laser fabrication is polishing the thin gain layer. After suitable laser-grade raw material is procured, the doped layer must be polished to very precisely controlled thickness. In addition, the polishing process should produce good surface flatness on both sides, good parallelism with low irregularity, low surface roughness, and negligible surface/subsurface damage. Example laser host crystals for thin disks are YAG, YVO_4, Lu_2O_3, Sc_2O_3, Y_2O_3, KGW, and KYW. Because it is one of the most commonly utilized materials, in the following sections we discuss the essential attributes of polished yttria alumina garnet (YAG) wafers for disk lasers.

2.1. Ceramic versus crystalline materials

Most current disk laser designs use either single crystal Yb:YAG or ceramic Yb:YAG as the starting material for the gain layer. The Yb:YAG doping concentration can vary from 1% up to 100%.[1] In some designs (see Fig. 1), an undoped YAG heat spreader cap of crystalline or ceramic material is bonded to the gain layer. Whether using crystalline YAG or ceramic YAG, it is very important to carefully specify and inspect for laser-quality bulk material prior to starting any fabrication steps such as grinding or polishing. In addition to possessing the standard requirements on laser-grade material to be free of voids and inclusions, YAG bulk material for disk lasers also must be carefully selected to have low birefringence and good index uniformity.

For making disk laser structures, one common practice is to purchase raw material in cylindrical rods. The rods are typically core-drilled to 10- to 20-mm diameter from a larger-diameter, single-crystal YAG boule. To avoid stress birefringence problems, the drilling sites should be selected based on the available stress-free or low-stress zones in the YAG

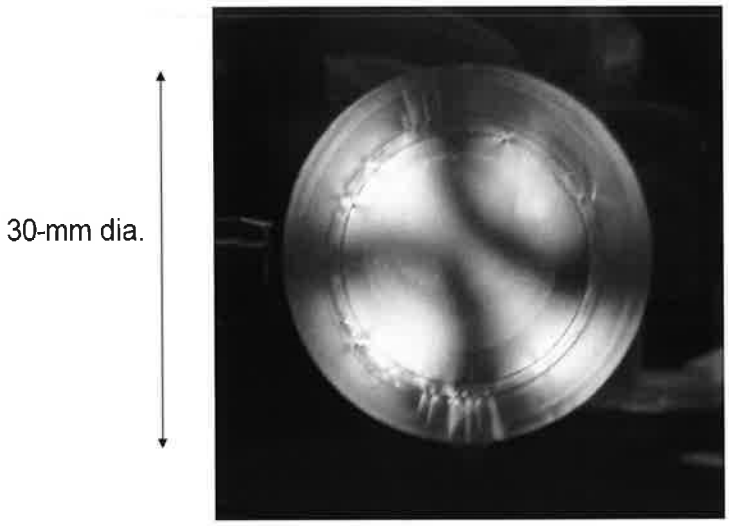

Fig. 2. Undoped YAG rod 150 mm long × 30 mm diameter, viewed through crossed polarizers. Intense, spatially variable birefringence pattern is due to stress in the original crystal boule.

boule. Lower stress zones can be identified by polishing the boule ends and illuminating the structure with white light between crossed polarizers (see Fig. 2). After core drilling, the rods may be annealed to reduce stress and then measured for extinction ratio (ER).

Ideally the cored-out rods should have low enough birefringence to produce a crossed-polarizer ER $\geq$ 1000 at 1064 nm. YAG suppliers generally will provide ER measurements at 633 nm, which is actually a more stringent requirement since the retardance of a given birefringent material scales inversely with wavelength as roughly $(1/\lambda)^x$, where $x > 1$. This scaling of the retardance comes from an explicit $1/\lambda$ dependence as well as some dispersion in the stress-optic coefficients that contribute to the retardance.[2] Cylindrical rods that pass the ER > 1000 requirement may be sliced into thin wafer stock before starting to mill, grind, and polish the disks.

One may argue that the extremely thin form factor of YAG disk lasers reduces the requirement for low stress birefringence in the raw material. However, we have seen that stress birefringence can also be correlated with refractive index inhomogeneity, which is possibly an even greater problem for thin disk laser design. An example of index nonuniformity can be seen in Fig. 3, which shows a set of YAG disks on a polishing plate. Since index inhomogeneity translates into optical-path length variations and transmitted wavefront error, one cannot correct the problem by polishing the two faces of the disk to be flat and parallel to each other.

Ceramic or polycrystalline YAG is also sometimes used for disk laser construction. While ceramic YAG bulk material may have less variation in stress birefringence across the bulk due to its different growth process and geometry, the bulk material still possesses a non-zero level of birefringence that can be problematic. However, we have not seen any evidence for a difference in the number of bubbles/inclusions when comparing ceramic to crystalline YAG, as both materials can be made essentially void-free. Due to excellent

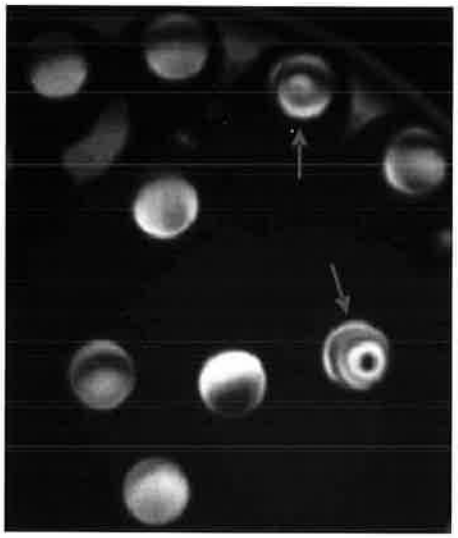

Fig. 3. Interferogram of crystalline Nd:YAG disks, <1 mm thick and 12.7 mm diameter, after polishing. All disks in the image have very flat and parallel surfaces. Red arrows indicate disks with high levels of internal index inhomogeneity.

sintering and HIP (hot isostatic pressing) processes used in ceramic YAG fabrication, there is no discernible grain structure in polished ceramic YAG surfaces.

Ceramic YAG is grown in large slabs with maximum width of 60 mm and maximum thickness of 10 mm, while the length of the slabs can be extended up to at least 200 mm. Due to the as-grown slab form factor, the most practical way to make disks from the available ceramic material is to core drill rods (10 mm long) out of the slab, and then slice them into wafer stock. One advantage that ceramic YAG possesses relative to crystalline YAG is the possibility of core drilling very large diameter rods (up to ~50 mm) with fairly uniform stress properties. This larger diameter availability makes ceramic YAG attractive for some wide aperture disk laser designs. Currently, there is only one reliable supplier of ceramic YAG in the world: Konoshima Chemical Company located in Japan, whereas there are several crystalline YAG suppliers in the U.S., such as Scientific Materials, VLOC, and Northrop Grumman Synoptics.

2.2. Thickness control

The thickness tolerance of the gain layer is an important specification for any solid-state laser design. While both precise mechanical and optical based measurement tools are readily available on the market, PPC prefers to use a proprietary scanning laser interferometer system dubbed the Sweepmeter to infer the thickness of plano/plano, parallel, polished YAG disks. Accuracy of the thickness determination can be as low as 100 nm, which is limited primarily by knowledge of the YAG refractive index over the scan range of the laser. One advantage to an optical measurement tool is that no mechanical contact is required. Disks can be measured throughout the polishing process as soon as they are transparent and

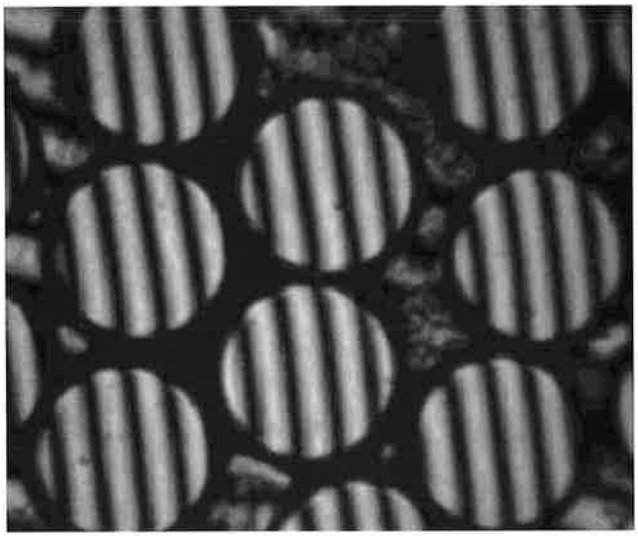

Fig. 4. Surface interferogram of multiple 14 mm diameter Yb:YAG disks that are blocked onto a polishing plate and have one side polished into a flat plane, shown by the straight, parallel interference fringes.

parallel enough to generate an etalon signal for the scanning laser. Using this metrology tool allows one to achieve submicron control over the thickness of an entire polishing block of YAG. While most thin disk laser designs do not require a thickness tolerance any less than ~5 μm, more precise metrology tools can be very useful in checking the wedge across a single YAG disk. In addition, interferometric-based optical measurement techniques can be made insensitive to systematic thickness offsets from blocking adhesives used to attach the YAG disks to the polishing plate.

2.3. Surface flatness

To obtain good surface flatness or a flat surface figure, it is essential to use a proper means of fixing the raw disks onto a flat, solid-glass plate or polishing block. The method for blocking should minimize stress to the parts and provide sufficient support to prevent them from moving during subsequent operations (see Fig. 4). Achieving good surface flatness depends on a succession of material removal steps, such as coarse milling, fine grinding, and polishing. Polishing can also be broken down into rougher and finer steps with different slurries being used in each step.

In general, the abrasives used to remove material and planarize the surfaces are applied in order of roughest (larger particle size) at the early stages of polishing to finest (smaller particle size) in the final stages of polishing. By applying careful attention to the mechanics of the polishing process, one can achieve flatness deviations of <0.05 waves peak to valley over a 90% clear aperture on a single disk. Fig. 5 demonstrates this kind of excellent surface flatness on a disk that is still attached to a polishing block. In this case, the disk surface takes on the same flat shape as the supporting plate, which can be made very flat

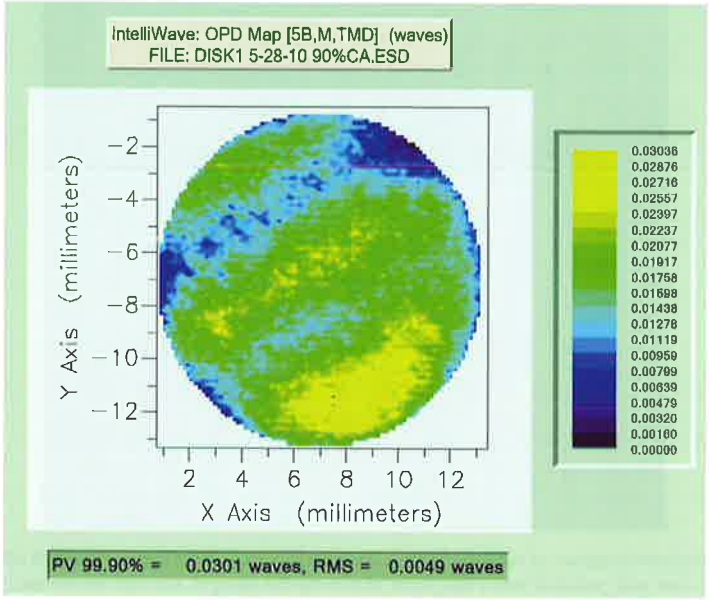

Fig. 5. Surface figure over 90% clear aperture (CA) of single, 14-mm diameter Yb:YAG disk on same polishing plate as Fig. 4. Flatness deviation is 0.03λ peak-to-valley (p-v) at 633 nm.

due to its much larger diameter compared to an individual YAG disk. Note that there is very little edge roll-off or rounding in the disk from Fig. 5, which also maximizes the usable aperture of the optic.

After polishing of the first disk surface is completed, the disks must be flipped over to repeat the process on side 2. Next the disks can be de-blocked or removed from their polishing block and flatness of the surfaces can be measured again. In most cases there is some change in surface flatness of a typical polished disk after it is de-blocked from the polishing plate. When the disk is no longer constrained by its adhesion to the polishing plate, it can relax slightly to a new equilibrium flatness that is determined by a very slight, built-in asymmetry between the polishing stress in the two surfaces (see Fig. 6). The free-standing disk in Fig. 6 has relaxed from 1/20 or 1/10 wave flatness deviation (as measured when it was attached to the polishing block) to roughly 1/2 wave flatness deviation with a primarily cylindrical shape.

2.4. Transmitted wavefront error (parallelism)

Another critical parameter for disk laser performance is parallelism of the two disk surfaces. Parallelism can be defined in terms of linear wedge, refractive (spherical) power, and higher order irregularity. To achieve good performance, the YAG layers are required to have wedge angles of <10 arc s or even <5 arc s in some cases. The best way to characterize wedge is via Fizeau fringe maps (also called TTV [total thickness variation] fringe maps) or by successive Sweepmeter™ scans across the disk using a 1-mm laser beam. However, to

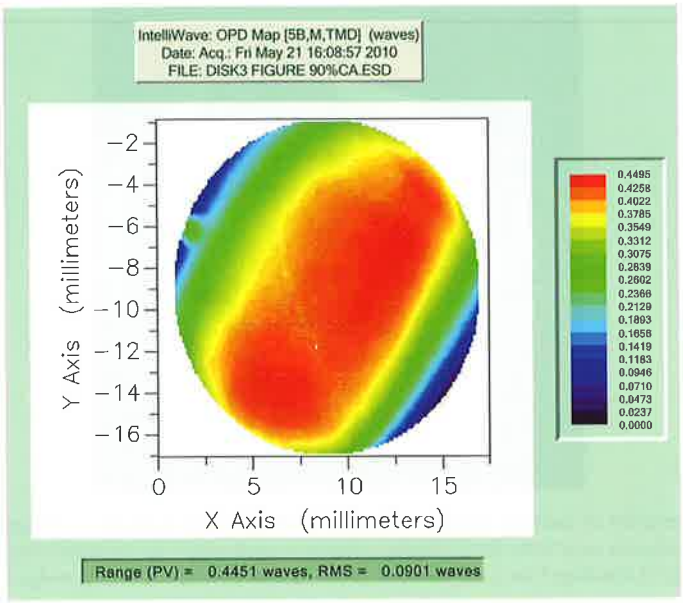

Fig. 6. Surface figure of free-standing, polished Yb:YAG disk, 18 mm diameter × 150 μm thick, 90% CA, after polishing both sides and deblocking from the polishing plate. Flatness deviation is 0.45λ p-v at 633 nm.

quantitatively measure refractive power and irregularity, measuring transmitted wavefront error (TWE) of a plane wave propagating through the disk is preferred. The TWE map can be fitted to a quadratic function to obtain the refractive power, while the residuals from the fit provide a measure of irregularity. Example measurements of high-quality YAG disks are shown in Figs. 7 and 8.

2.5. Surface roughness and subsurface damage

To achieve a high laser damage threshold in the coated interfaces and surfaces of a disk laser, the polished surface quality must be excellent. The surface should be free of macroscopic defects such as scratches and digs—most laser surfaces are required to have <10–5 scratch–dig by MIL-PRF-13830 or an equivalent standard. In addition, the surface roughness should be very low to reduce loss of light from scattering processes. While it is perhaps a matter for debate as to exactly what roughness threshold should be set for operation at the Yb:YAG laser wavelength of 1030 nm, most disk laser research groups require surface roughness of <10 Å rms and some designs even call for <5 Å rms. In practice, low surface roughness and minimal sub-surface damage go hand-in-hand because it is impossible to polish extremely smooth surfaces when there is underlying damage. If any microfractures or scratches extend downward into the surface from a previous, coarser polishing step, then the rms roughness will be suboptimal. For this reason, all subsurface damage must be cleaned away during subsequent fine-polishing operations. An example of a superpolished (<1 Å rms) surface is shown in Fig. 9.

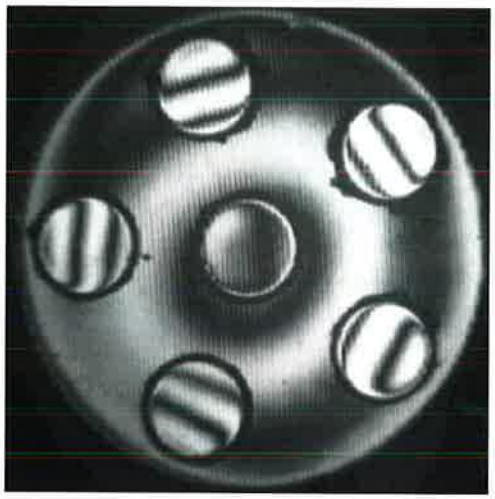

Fig. 7. Interferogram of polished block of five YAG disks, 15 mm diameter × 150 μm thick. Fizeau fringe pattern indicates outer disks have a wedge pointing toward center due to underlying shape of block. Maximum wedge is less than 5 arc s for the outer disks. Central disk has near-zero wedge.

3. Thin Film Coatings

Optical thin-film coatings are essential for a thin disk element's performance. They must offer good spectral performance and low scattering and absorptive loss, as well as having very high power/fluence–handling capabilities. For a structure such as the one illustrated in Fig. 1, a dielectric, high-reflection (HR) coating is used to reflect the lasing and pump

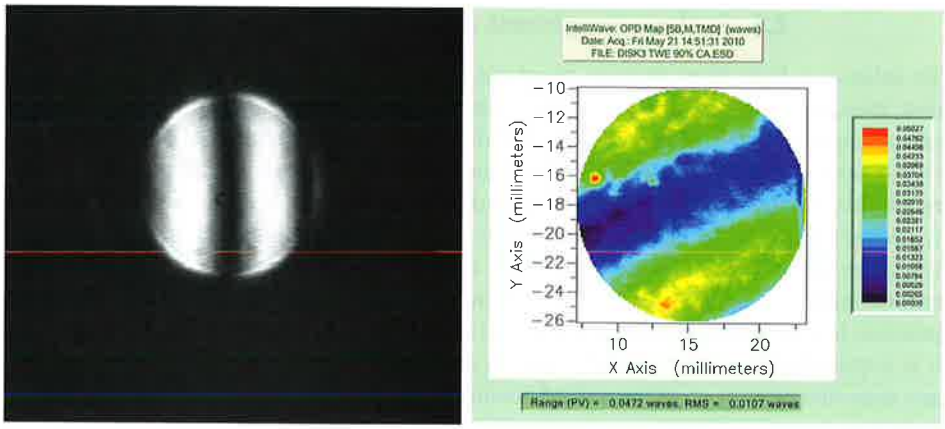

Fig. 8. *Left* image is an interferogram of an 18-mm diameter YAG disk showing the Fizeau fringes due to a small linear wedge in the horizontal direction. *Right* image is a TWE measurement over 90% CA on the same disk. TWE is <0.05λ p-v at 633 nm.

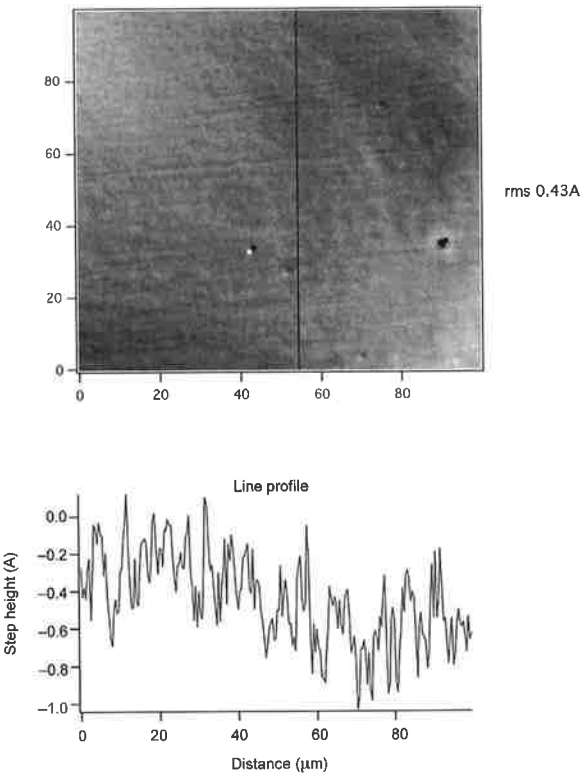

Fig. 9. Superpolished surface with rms roughness = 0.43 Å over 100 μm × 100 μm window, measured by Nomarski microscope. The defect at *right* was deliberately included to aid focusing on the fine surface texture in the surrounding area.

wavelengths at the bottom of the active layer. In addition, an antireflective (AR) coating is used to reduce the loss for the lasing and pump wavelengths at the air–structure interface. In addition to spectral performance of the coatings, other factors such as thermal conductivity, laser damage threshold, and coating stress have to be considered in the coating design.

3.1. Ion beam sputtering overview

The authors have found that ion beam sputtering (IBS) technology provides a combination of performance characteristics that are particularly well suited for thin disk applications. IBS optical coatings offer low scatter and absorption losses, superior durability, and environmental stability compared to conventional or ion-assisted evaporated coatings.[3] This makes them ideal for high-fluence, solid-state applications that face extreme temperatures or other environmental factors which can affect optical or mechanical performance.

During IBS deposition, an ion beam is created by generating plasma inside an ion source (Fig. 10). The ions are accelerated out of the source through a biased grid and

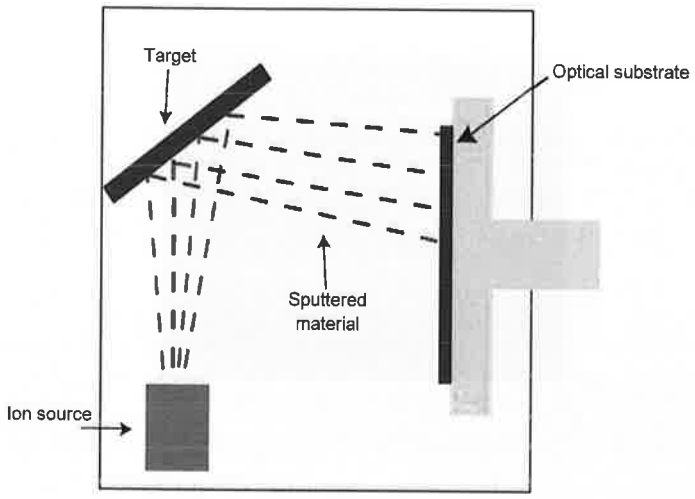

Fig 10. Layout of typical IBS coating chamber.

aimed at a coating material target. The ions sputter molecules/atoms from the target which then deposit on the substrate being coated. Some typical target materials are SiO_2, silicon, tantalum, titanium, hafnium, and niobium. When metal targets are being used, oxygen is introduced in the coating chamber during deposition so that the deposited material forms fully oxidized coating layers. Alternating layers of different coating materials are deposited by rotating different target materials into position during deposition.

The sputtering process transfers very high energies to the coating molecules. This gives the molecules great mobility as they arrive at the substrate surface, an essential aspect of achieving coatings with densities close to those of bulk material. In contrast, coatings deposited with electron beam (e-beam) deposition have much lower energies resulting in porous coatings that are susceptible to moisture shifts and are mechanically less durable.[4]

The IBS coating process is also fully automated, resulting in excellent run-to-run repeatability and spectral performance very close to the theoretical design. Combined with the low loss levels and environmental stability of the coating layers, very tight optical specifications can be achieved such as AR coatings with $R < 0.05\%$ and sharp transitions on long/short-wave pass–types of coatings.

An additional benefit of IBS coatings are that the internal stress in the coatings is stable over time straight out of the coating chamber and can easily be modeled. This makes stress management of the coatings much easier than for e-beam coatings where the stress, although lower than for IBS coatings, changes over time and is influenced by relative moisture in the environment. A comparison of typical properties for different coating technologies is shown in Table 1.

3.2. Typical spectral designs and design considerations

If we consider an example of an Yb:YAG active layer lasing at 1030 nm and pumped at 941 nm, a simple HR coating stack centered at 1030 nm will not cover both 941 nm and

Table 1. Typical parameters for selected optical coating deposition processes

	Electron beam evaporation	Ion-assisted deposition	Magnetron sputtering	Ion beam sputtering
Deposition rate	>10 Å/s	~10 Å/s	~10 Å/s	~3 Å/s
Coating area per run	1256–4400 cm^2	1256–4400 cm^2	>4400 cm^2	650–1250 cm^2
HR LDT (1064 nm HR, 20 ns, 20 Hz)	~5–30 J/cm^2	~5–30 J/cm^2	~10 J/cm^2	>40 J/cm^2
Absorption	>100 ppm	>50–100 ppm	10 ppm	<2 ppm
Thermal conductivity	Low	Medium	High	High
Temperature range	~300 °C	~300 °C	~300 °C	–196 to >500 °C
Number of layers	1–50	~50	~50–100	>200
Surface roughness/ scatter	+10 Å rms	+8 Å rms	<5 Å rms	<1 Å rms (conformal)
Density/porosity	Porous	Dense	Near bulk	Near bulk
Adhesion/durability	Low	Good	Very good	Excellent
Humidity sensitivity	Yes	Yes, small	No	No
Aging effects	Yes	Yes, small	No	No
Intrinsic stress	<100 MPa	~100 MPa	Few 100 MPa	Few 100 MPa
Wavelength range	193–10,000 nm	200–10,000 nm	250–3000 nm	250–5000 nm

Note: These values are typical values indicative of average industry standards. They in no way represent a specific supplier and exceptions may exist.

1030 nm. One option is to center the coating halfway between the two wavelengths. This works well if the bandwidth of the HR coating covers the 941- to 1030-nm range. This is the case for a typical Ta_2O_5/SiO_2 quarter-wave coating stack, but requires good centering of the coating (Fig. 11). The coating thickness for this design is ~5 μm. Typical reflectivity of >99.9% is readily achieved.

The situation becomes a bit more complicated if the disk laser is operated with the pump and/or the lasing light incident at a non-normal angle of incidence (AOI). The main effect on the coating is to shift the coating curve to shorter wavelengths as the AOI increases. It is therefore easy to design the coating for the case where 1030 nm is close to normal AOI, and the 941 nm is at a larger AOI. A HR-coating design centered at 1030 nm will shift shorter and be centered at 941 nm at 22.5 degrees internal AOI in YAG (corresponding to ~44 degrees external AOI) (Fig. 12). Lower AOI for 941 nm can also easily be accommodated by reoptimizing the centering of the coating design.

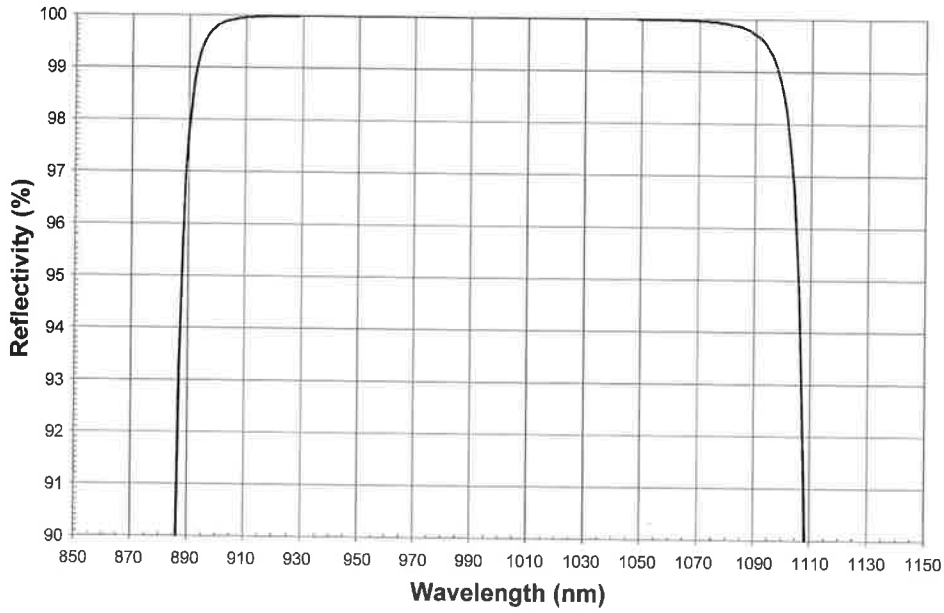

Fig. 11. Modeled reflectivity of a quarterwave, Ta_2O_5/SiO_2, high-reflector coating stack centered to cover both 941 nm and 1030 nm.

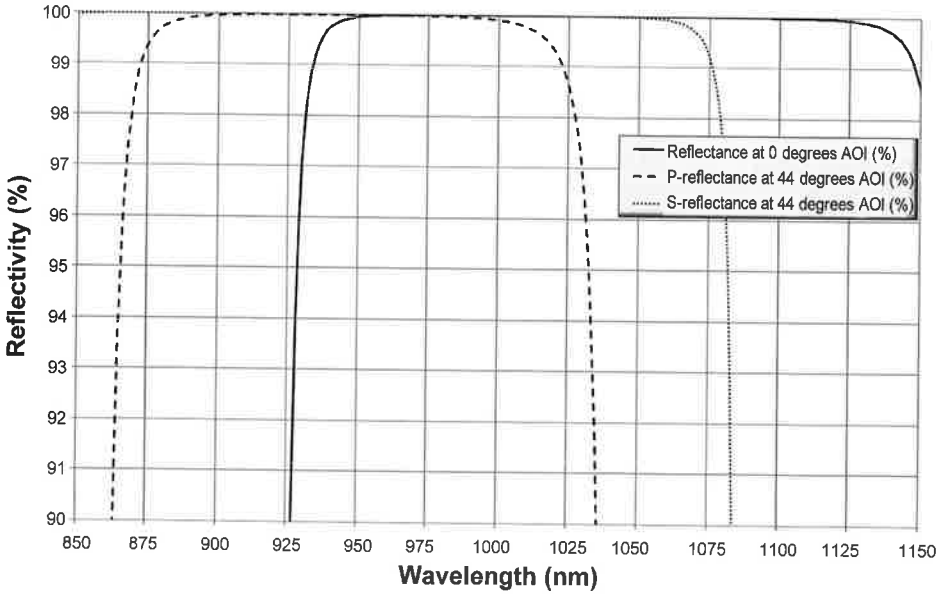

Fig. 12. Modeled reflectivity of a quarterwave Ta_2O_5/SiO_2 high-reflector coating stack centered at 1030 nm at 0-degree AOI showing how it shifts to shorter wavelengths and centers at 941 nm at 44-degrees external AOI on YAG. The dotted and dashed lines are for p- and s-polarization, respectively.

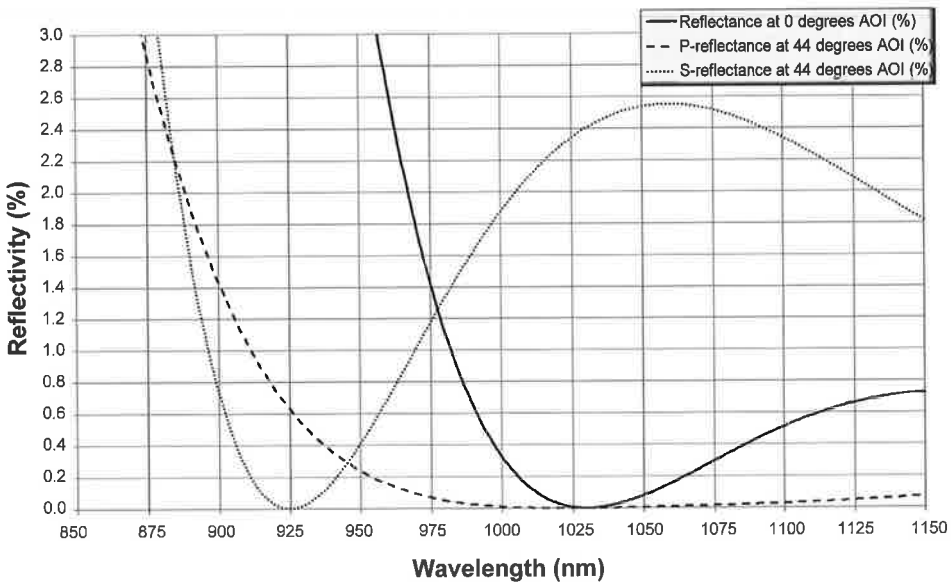

Fig. 13. Modeled reflectivity of an AR coating optimized for 1030 nm at 0-degree AOI and at 941 nm at 44-degree external AOI in YAG. The dotted and dashed lines are for p- and s-polarization, respectively.

The AR coating needs to have low reflectivity for both the lasing and the pump wavelengths. This is achieved with a relatively simple dual-band coating design. Typically, the lasing wavelength performance will be prioritized and optimized to obtain reflectivity levels below 0.1%. The thickness for the AR coating is in the 0.5- to 1.0-μm range, depending on design details. An example design for a 1030-nm AR at 1030 nm and 0 degrees, and 941 nm at 44 degrees external AOI on YAG is shown in Fig. 13. Different AOI configurations can easily be accommodated by reoptimizing the design.

3.3. Laser damage resistance

Due to the high laser fluences generated in thin disk laser structures, laser damage resistance of the optical coatings becomes critical. Factors influencing the laser damage threshold (LDT) of the coated interfaces include surface defects, roughness levels, absorption levels, and coating material structure and defect levels. For high average power, absorption is the leading driver for damage, while for pulsed operation with high peak electric fields, defects leading to field enhancement are the driving factor.

To obtain the highest LDT possible, all of these factors have to be addressed starting with preparation of the surface to be coated. As described above, the surface has to be polished to laser-grade finish with minimal subsurface damage, digs, and scratches, and must have low rms surface roughness. The surface then is thoroughly cleaned prior to coating, and is handled throughout the coating process without introducing particulates that can create defects in the coating. This handling process is similar to how wafers are processed in a semiconductor fabrication environment.

Ion beam sputtered coatings are particularly well suited to handle high average power due to the low absorption levels (1–2 ppm range). LDT greater than 15 MW/cm^2 for cw applications has been reported.[5] For pulsed operation, LDT of over 40 J/cm^2 (20-ns pulse length, 20-Hz repetition rate) has been achieved.[6]

3.4. Coating stress management

The active layer of a thin disk laser is thin compared to its diameter. Deposition of an optical coating on one of its surfaces will introduce a deformation to the active layer. If the deposited coating has compressive internal stress, the coated surface will end up convex, while a coating with tensile stress will result in a concave surface. For a 15-mm diameter disk with 200 μm thickness, the IBS HR coating design shown in Fig. 12 will result in a convex surface with over 30 waves (at 633 nm) of sag. The deformation is mainly in the form of spherical power.

There are different approaches to deal with this deformation from coating stress. One is to bond the active layer so that it conforms to a more rigid, thicker substrate. This is difficult to achieve with glue as the glue layer prevents good conformation between the active layer and the substrate. Direct bonding (such as PPC's CADB® process) is better suited to achieve conformance.

It is also possible to address the stress by compensation. If both sides of the active layer are coated (e.g., the AR–HR configuration described above) the two coatings can be designed to match each other's stress so that the overall stress is balanced. Coating stress compensation can be done quite reliably with IBS coatings since the coating stresses are well characterized, stable[2] and repeatable; that is not the case for conventional e-beam coatings.

3.5. Environmental robustness

The optical coatings in a thin disk structure have to be environmentally robust. This is true in particular for configurations involving fluid cooling directly to the back of the HR coating; the coating has to withstand erosion from the cooling fluid flow.

In addition, the coatings have to be resistant to thermal stresses generated during operation. For designs where cooling is achieved by soldering the thin disk laser to a heat sink, the coatings have to withstand the thermal stress encountered during the soldering process. Again, higher energy deposition processes such as ion beam sputtering seem to be best suited to these requirements.

4. Bonding and Assembly of Heat Spreader Caps

The capped or heat-spreader design is becoming more widely utilized in thin disk lasers. The cap is typically made of a high-conductivity material like sapphire or an undoped version of the host material to allow for a proper coefficient of thermal expansion (CTE) match. It helps minimize thermal distortions of the gain media when using end-face pumping or in certain cooling regimes.[7] Because the pump light is being transmitted through the cap, any absorption or scattering of light at the interface will cause adverse effects on performance. In addition, if the assembly process results in distortion of the thin-disk gain media, beam

quality can also suffer. Because of these factors, almost all current, capped thin disks are assembled with an epoxy-free bonding process.

4.1. CADB® overview

While there are several alternative processes to epoxy bonding now commercially available, such as those offered by Onyx Optics and the Stanford patented process used by companies such as VLOC, Precision Photonics Corporation (PPC) exclusively utilizes the Chemically Activated Direct Bonding Process (CADB).[8]

With CADB, the parts are polished and physical and chemical contaminants removed. The surfaces are then chemically activated utilizing a proprietary chemical treatment to increase the density of available bonds at the surface. The two parts to be bonded are brought into contact with each other, at which point the outer molecules from each surface bond together. CADB has been successfully used for a variety of applications, including composite bonding of dissimilar materials, in which it is typically only limited by the mismatch of the coefficient of thermal expansion of the materials.

CADB technology results in epoxy-free optical paths that are 100% optically transparent with negligible scattering and absorptive losses at the interfaces. It offers bond performance equivalent to that of the bulk materials being bonded, and has been proven to be exceptionally durable, reliable, and resistant to laser fluence, temperature, and humidity.[9] It has therefore become widely utilized as an epoxy-free assembly process for solid-state laser crystals in high-fluence and other aggressive environments.

In the following we review bond strength, fluence handling capability, and other key properties of this technology.

4.2. Bond strength

Bond strength is obviously a key parameter in evaluating any novel assembly method. As many solid-state lasers are deployed in the field or utilized in space flight applications, the core optics must be able to withstand notable shock, vibration, and temperature fluctuations. In addition, bulk-like material properties allow for extensive postprocessing of the bonded assembly—necessary for certain more elaborate designs. In our most recent work, we demonstrated bond strength exceeding bulk strength for bonded samples of common laser materials such as YAG, phosphate glass, and fused silica.[10] A summary of that work is given below.

Bulk samples were prepared by taking raw material samples of Qx/Er phosphate glass, ceramic YAG, and fused silica, polishing them to a thickness of 7 mm and dicing them into squares that were slightly oversized from 3 mm × 3 mm. Samples were then polished on all four sides to achieve a laser-quality finish. The sharp corners had a slight bevel applied to break any sharp edges. To ensure that all surface damage was eliminated during the polishing, we removed at least 0.5 mm of material for each of the four outer surfaces. Surface roughness for all three materials was identical, in the range of 5 to 9 Å rms.

CADB samples were prepared in much the same way. For each material type, we used additional material from the same lot as the bulk samples. We polished two separate wafers to a thickness of 3.5 mm. These two wafers were bonded together using the CADB process. The resultant wafer assembly was then diced into dimensions slightly oversized

Fig. 14. Test fixture setup for sample fracture-strength measurements (phosphate glass sample is shown). (From Traggis, N., and Claussen, N., Improved bond strength characterization of chemically activated direct bonding (CADB) epoxy-free bonded solid state laser materials, SPIE Proc. **7578**, 75780F (2010).)

from 3 mm × 3 mm. Samples were then polished on all four sides to a laser-quality finish and the corners had a slight bevel applied to break any sharp edges. Again, surface roughness for all three materials was identical, in the range of 5 to 9 Å rms. These samples were therefore identical in every manner with the exception of the bond line in the CADB samples.

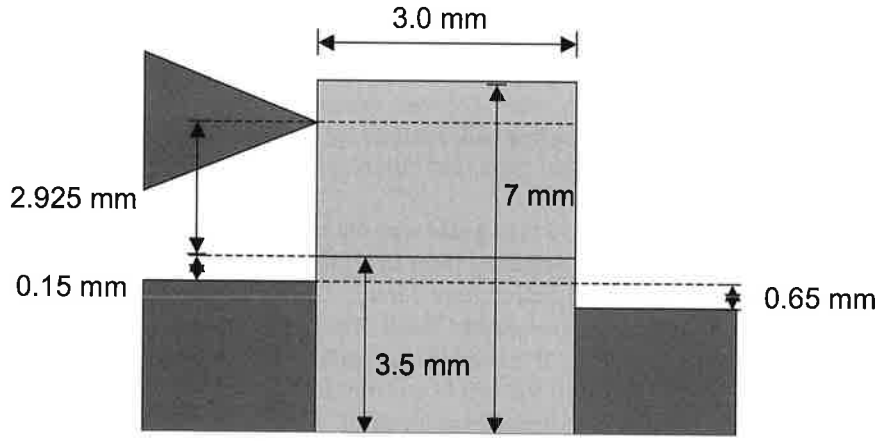

Fig. 15. Schematic with exact dimensions for sample fracture–strength measurements. (From Traggis, N., and Claussen, N., Improved bond strength characterization of chemically activated direct bonding (CADB) epoxy-free bonded solid state laser materials, SPIE Proc. **7578**, 75780F (2010).)

Table 2. CADB-bonded and bulk material strength for ceramic YAG, Qx/Er phosphate glass, and fused silica samples

	Qx/Er phosphate glass	Ceramic YAG	Fused silica
Bulk samples	10.5 (0.6) kg	28.9 (1.6) kg	8.5 (0.5) kg
CADB bonded samples	11.3 (0.7) kg	30.7 (1.1) kg	9.6 (0.5) kg
Ratio (% of bulk strength)	108(9)%	106(7)%	113(9)%

Source: Traggis, N., and Claussen, N., SPIE Proc. **7578**, 75780F (2010).

Samples were then constrained in a test fixture under equal load and a force was applied to them at the same height in every sample. This force was applied until fracture was observed and the peak force was measured via an Imada DPS-110 load cell. Each sample set consisted of 10 to 20 identical pieces. Testing of all sample sets was performed at the same time, and by the same operator to help ensure consistency of results. A picture of this test fixture is shown in Fig. 14, and a schematic with exact dimensions is shown in Fig. 15.

A summary of the average strength results for each sample set is shown in Table 2. For each material type, we observed that the CADB-bonded samples tested to a slightly higher average force than the bulk samples. However, the authors would point out that this difference is within the noise of the measurement. While there are reasons that the CADB process may in fact strengthen the samples, it is sufficient to say for now that the CADB-bonded samples achieved similar strength values to those of the bulk. This is validated by a visual inspection of the fracture surfaces where the CADB samples and the bulk samples appear to be identical in fracture type and propagation.[10]

It is also worth pointing out that bulk material strength increased over previous work when the surfaces under test were polished.[10,11] These results can be explained in terms of a well-known relationship of brittle materials. Previous studies of brittle materials have demonstrated that fracture stress is inversely proportional to the square root of the length of a surface crack.[12] As the surface fracture grows in length, the stress required to break the sample decreases. We estimate that the size of surface fractures/damage on a diced surface is 50 to 100 μm, whereas surface fracture/damage depth is reduced to a negligible level (<1 nm) after polishing. This simply emphasizes that polishing quality and method are also important for mechanical robustness and not just optical performance. This is something to be considered when designing an optic!

4.3. Laser damage threshold

The laser damage threshold of the bond interface for a heat spreader capped device is very critical as both the pump light and output light are transmitted through this interface in a typical face/end-pumped configuration. LDT can be impacted by both absorption and scattering at the interface so a very high quality polish is critical for any surfaces to be bonded, as discussed previously. While very preliminary LDT studies of a standard CADB interface for both ceramic and single crystal materials have been published, the most relevant data comes from customers testing under actual operating parameters.[9] In 2009, Boeing LTS /AFRL demonstrated 6.5 kW of output power at 1030 nm from a single, capped thin disk element bonded using the CADB process. This device was pumped at 12.7

kW over a 2.54-cm^2 area, resulting in the bond interface being exposed to a power density of ~5 kW/cm^2, without any observable degradation at the bond interface.[13] The authors have found that LDT seems to be limited by factors such as surface and subsurface damage and contamination at the interface (similar to those factors impacting LDT of thin film coatings), and will continue to work with laser builders in testing under actual application conditions and documenting and improving upon appropriate performance expectations in this regard.

5. Bonding and Assembly of Thin Disk to Heat Sinks

Thin disk lasers are thermally advantageous due to the inherent proximity of the gain medium to the heat sink, and the control over the direction of heat flow relative to laser beam propagation. Temperature gradients created by a good pump configuration are typically coaxial to the laser beam propagation and therefore contribute minimally to beam aberrations.[14] To realize these advantages in practice, the mounting considerations of the thin disk must be carefully considered. Primary heat removal and mounting considerations for the disk-to-heat-sink interface material are the following:

- Maximize thermal conductivity
- Minimize total thickness, to optimize/maintain pure one-dimensional heat flow
- Maintain thickness uniformity across the disk surface
- Avoid or control shrinkage during cure, if an adhesive or epoxy
- Consider compliance/elasticity/elongation for the interface
- Consider the coefficient of thermal expansion (CTE), and its match to the CTE of the thin disk structure and heat sink material
- Maximize reliability of the interface material, and reproducibility of the attachment method
- Design for the full operational temperature range

In this section, details of proper disk mounting will be discussed, as well as several techniques that have proven successful.

5.1. CTE and conductivity considerations

Figure 1 shows the many layers that must be considered for a mounted thin disk. Each layer has a CTE and associated thermal conductivity. There may be even more layers, depending on the interface material and heat sinking method. The first aspect to consider is the choice of laser gain medium or laser crystal. This affects many factors in the overall design because the CTE for the crystal will impact material choices for all other layers. An effective heat spreader or ASE cap on the top side of the active layer works best with a close CTE match to the laser crystal, as this allows an optical contact to be used rather than adhesives. Similarly, it is advantageous to choose a heat-sink material with CTE close to that of the laser crystal. Example heat sink materials are copper, aluminum, copper tungsten, tantalum, and other various alloys. Keeping with YAG as the example host medium, with CTE ~8 ppm/K, good choices for heat-sink materials would be copper tungsten alloys (CuW) or tantalum metal, as shown in Table 3. Depending on the operational temperature range and the storage temperature range, it may also be beneficial to consider the CTEs for the thin film materials used in the AR and HR coatings.

Table 3. Thermal conductivities and thermal expansion coefficients for relevant thin-disk mounting materials

	Example solders				Example heat sinks				Example epoxies, adhesives
Material	Single-crystal YAG[15]	CuW90[a]	CuW85[a]	Ta[16]	Silver-alloy/liquid metal[20]	Thermally filled epoxy[b]	Boron conductive adhesive[17]	Indium nitride-filled adhesive[18]	Gold-solder[16]	Eutectic tin solder[19]
Thermal conductivity (W/(mK))	12.9	180~190	190~200	57.5	0.5–10	1.0	1.5	81.6	57	16.5
Coefficient of thermal expansion (10^{-6} K^{-1})	7.7–8.2	5.6~6.3 (20–100 °C)	6.3~7.0 (20–100 °C)	6.3	–	31	Compliant silicone	32.1, somewhat compliant	16	Liquid

[a]Data from material manufacturer Martech International Inc. (www.Marchtech-metals.com).
[b]Range from data sheets of various silver epoxy manufacturers.

5.2. Epoxies and adhesives

The next step to consider for thin disk mounting is the choice of material for mounting the disk to the heat sink. The simplest choice is an adhesive or epoxy, and in many cases the use of a relatively low thermal conductivity material for the interface is acceptable, particularly when the average power is low or the interface can be made extremely thin.[21] Table 3 indicates that some of the most popular thermal adhesives have dramatically lower conductivity than the crystals or heat sinks. It is absolutely essential to keep such layers as thin as possible to reduce the overall thermal impedance. Typical choices for such adhesives begin with silver-filled epoxies, which can have conductivity approaching that of the laser crystal. These materials tend to be a paste, which can have air entrapment and it is challenging to achieve very thin layers. Another choice is to use a more standard two-part adhesive, with improved viscosity allowing thinner layers. This allows the use of lower intrinsic thermal conductivity for the interface material, while maintaining the overall conductance of the interface layer. This method can be quite robust, and reliable, but has thermal limitations in the highest power systems.

Both of the above epoxy examples tend to be fairly rigid, and provide precise positioning in a permanent sense. In some cases it is useful to have a thermal interface material with compliance, and allow the laser crystal to bend freely or otherwise distort without having the adhesive layer apply a substantial restoring force. This can be accomplished, for example, by using silicone-based adhesives with thermally conductive fillers.[18] The example in Table 3 shows that such adhesives have fairly low thermal conductivity, but have the advantage of substantially lower stress transmitted to the laser crystal. In situations where it is desirable to allow the crystal to freely distort, a compliant interface may be critical.

5.3. Solders

Higher-performance interfaces necessarily involve higher thermal conductivity materials. Various soldering processes have been proven with thin disk lasers, particularly pure indium solders. Because of the relatively soft nature (low tensile strength) of pure indium, a soldered indium interface remains somewhat compliant over a very wide temperature range, and can deform to absorb stresses within the solder layer. This allows a CTE mismatch between the laser crystal and heat sink to be accommodated without severely compromising thermal conductivity. Indium solder can have one to two orders of magnitude larger thermal conductivity, relative to adhesives or epoxies. Typically, surfaces to be soldered will be prepared with a stack of metallic coating layers, including a "sticking" layer such as titanium or chromium, a "blocking" layer such as platinum to prevent solder migration and contamination of the interface, and a "sacrificial" layer such as gold to improve the wetting and adhesion of the soldered surfaces. A typical stack is ~0.1 μm of Ti, ~0.1 to 0.2 μm of Pt, and ~0.2 to 0.5 μm of Au. These layers are applied to the laser disk structure and the heat sink, prior to soldering. Final indium solder thickness can vary from ~10 μm to 300 μm (Fig. 16).

Cleanliness of the surfaces is essential, and often the soldering is performed in vacuum or an oxygen-free environment to further improve wetting and adhesion. For optical assemblies, the liquid flux that is used to remove solder oxides for efficient wetting is usually not allowed. Such fluxes can lead to contamination from organic residues, and flux residue removal can sometimes be challenging for optical surfaces. Because of this,

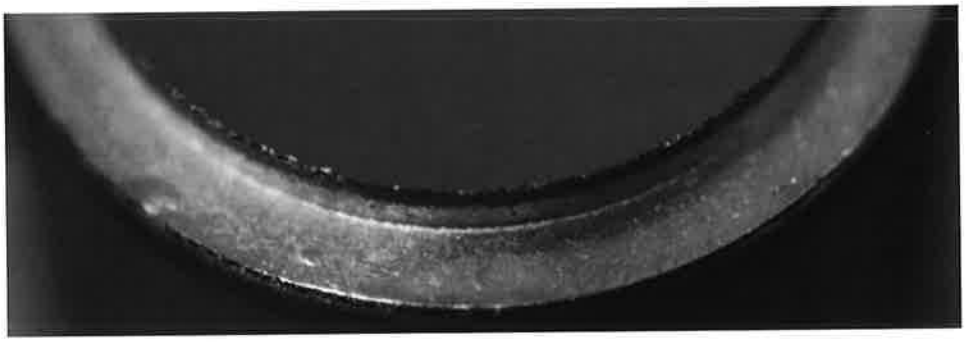

Fig. 16. Close-up view of a soldered thin-disk structure, showing the heat sink, thin solder layer, and some residual overspray of the Ti:Pt:Au layers on the edge.

fluxless soldering is preferred for thin disk-laser assemblies, and the procedures closely follow those established by the optoelectronics/photonics packaging industries.[22,23]

Fluxless indium soldering has several known limitations, however, such as high cost, large creep rate, poor corrosion resistance, and high thermo-migration rate. For many high-reliability applications, indium solder is replaced with a more robust "hard solder" such as eutectic gold-tin (AuSn20). Here the conductivity is reduced somewhat, but the CTE match is improved, while long-term reliability is improved and creep is eliminated.[24] The use of noncompliant Au–Sn solders requires a better CTE match between the laser crystal, heat sink, and solder in order to be effective, and a tailored cooling profile can reduce final stresses. Au–Sn solder tends to transmit stresses from the CTE mismatch to the optical part, which can lead to wavefront aberrations in the laser, and those stresses can also lead to fatigue-type failures over repeated temperature cycles.

5.4. Other disk-mounting methods and thermal materials

There are laser configurations where the compliance of an indium-soldered interface is not enough. In those situations, a page can be taken from the electronics manufacturers' toolkit, and the use of low-melt alloys,[20,25–27] or so-called liquid metals, can replace solders. This low-stress mounting technique has been proven for slab lasers[28] and could also be applied to disk lasers.

Another configuration uses pressure clamping to help maintain a flat optical surface for the disk laser, which can alleviate some of the wavefront aberrations from nonuniform thermal loading. This has been demonstrated with directly applied pressure from a sapphire plate.[29] A variation of this method uses a built-in microchannel cooler as the heat sink surface, and pressure clamping from a hydrostatic pressure differential between the surrounding atmosphere and the coolant fluid in the microchannels.[30]

Diamond has been investigated as a heat spreader for various rare-earth–doped disk laser designs,[31,32] and can be incorporated on the cooling side, the pumping side, or both. Similarly, silicon carbide has been used as a heat spreader,[33] with nearly equivalent performance for diamond and a smaller CTE mismatch between materials. Similar approaches are being used for optically pumped semiconductor lasers (OPSELs or VECSELs).[34,35] Whether semiconductor disk or rare earth–doped disk, birefringence in the diamond heat spreader

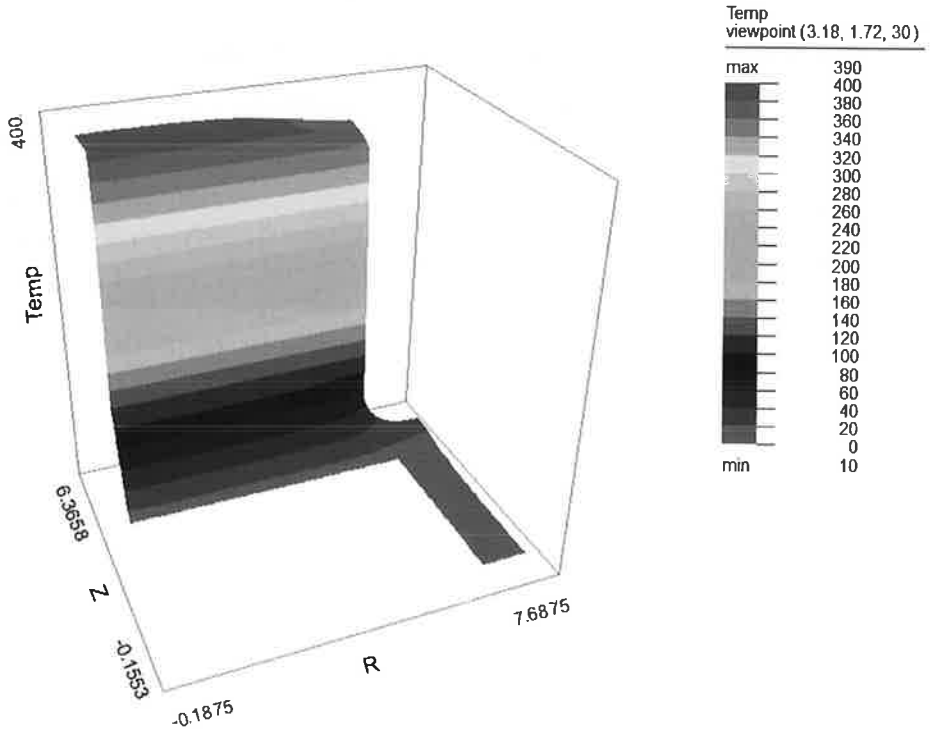

Fig. 17. Temperature distribution (°C) calculated using finite element thermal modeling for a soldered thin-disk laser mount with a 100-kW/cm³ heat load in a 200-μm thick Yb:YAG gain layer, a 1-mm thick undoped YAG cap soldered to a 1-mm thick, water-cooled CuW heat sink, and 10 °C water temperature. Z gives the position through the structure in millimeters from top to bottom (zero is defined to be on the top of the undoped YAG cap), and R is the radius from the center of the structure in millimeters. (Thermal modeling performed by Vern Schlie of Integral Laser Solutions.)

is a concern, and can limit performance.[36] Work in this area is quite active, and the major concern is robustness of the contact between the active gain layer and the heat spreader. Because the CTEs for SiC or diamond do not match most relevant laser materials, direct optical contacting is challenging. Thin adhesives or weaker optical contacts are used in that case. Heat spreaders of nearly identical material can be used instead, such as Cr:ZnSe sandwiched between ZnSe disks, which eliminates the CTE matching issues and provides an ASE cap as well.[37]

5.5. Direct glass-to-metal bonding

PPC has also investigated a method of directly bonding the laser gain media to a metal/metal alloy heat sink using its CADB technology. As discussed earlier, CADB interfaces are durable, and resistant to changes in laser fluence, temperature, and humidity. Due to the zero

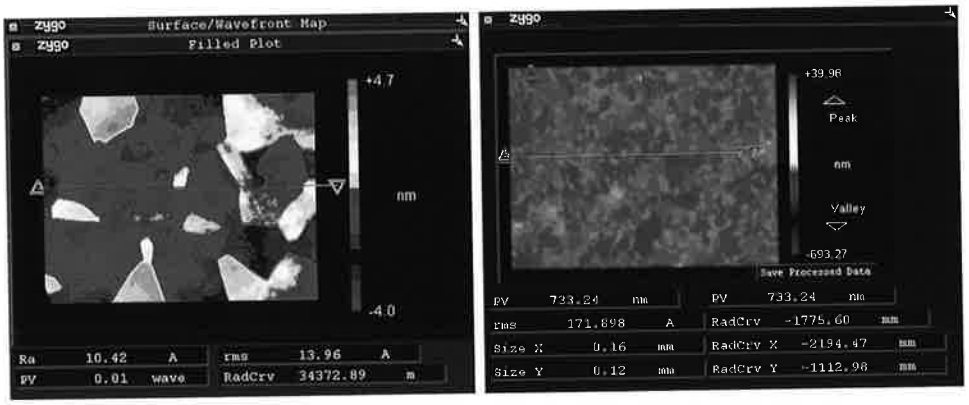

Fig. 18. Typical small aperture interferograms of the polished tantalum (left) and CuW (right) surfaces.

bond-line thickness, complete conformance is ensured between the two bonded surfaces, eliminating possible sources of wavefront distortion and improving heat conductivity.

Finite element modeling has been performed to compare thermal performance of a soldered thin disk laser mount to a CADB interface. The resulting thermal distribution for the soldered mount is shown in Fig. 17 for a 100-kW/cm^3 uniform heat load in the active Yb:YAG layer. The Yb:YAG active layer was taken to be 200 μm thick, mounted on a 1-mm thick, water-cooled CuW heat sink with 10 °C water temperature. The diameter of the YAG and CuW were 12 mm and 15 mm, respectively. A 1-mm thick, undoped YAG cap was included on top of the active layer. A 5-μm thick indium solder layer was included in the structure together with a typical titanium-platinum-gold metallization coating. Only a small difference in maximum temperature was found between the indium soldered mount and a CADB mount. As expected, the heating is quite high for such a large heat load, predicting almost 400 °C on top of the structure and approximately 120 °C on top of the CuW heat sink (thermal modeling performed by Vern Schlie of Integral Laser Solutions).

It is clear from the large temperature gradients shown in Fig. 17 that matching of CTEs among the laser gain media, the heat sink, and the intermediate layer materials is important. As mentioned above, CuW composites are often selected as heat sink materials due to high thermal conductivity and good CTE match to YAG. In particular, 90% tungsten:10% copper (CuW90) and 85% tungsten:15% copper (CuW85) composites are used.

Direct bonding requires the surface of the heat sink material and the laser gain structure to conform to each other on a molecular scale. This is most readily achieved if both the heat sink and the gain material are polished optically flat. However, the CuW composite materials are hard to polish due to the local hardness variation between the tungsten and the copper domains, resulting in a high surface roughness. PPC has also studied bonding to tantalum metal as it is easier to polish and has a good CTE match to YAG. However, the thermal conductivity is less than a third that of the CuW composites (Table 3).

In a recent study at PPC, 1" diameter × 0.25" thick CuW90 and tantalum substrates were polished. The rms surface roughness in the 5- to 15-Å range was obtained on the tantalum substrates, although a grain structure was observed (Fig. 18). The CuW substrates

Fig. 19. CADB-bonded YAG-CuW structure (Sample C) with HR coating at the interface.

experienced differential polishing between the tungsten and copper domains resulting in almost 200-Å rms surface roughness. Fig. 18 shows a typical small aperture interferogram of the polished CuW surface. This high surface roughness would normally prevent CADB bonding to the substrates; however, PPC has developed a surface treatment process to overcome this issue.

For the bonding tests, laser-grade, crystalline YAG substrates polished to 3- to 4-Å rms surface roughness with laser-grade surface quality were used. The substrates were 1" diameter × 1.1 mm thick. Some of these substrates were coated with a high-reflection coating for 1030 nm (see Fig. 12) to simulate the material interface present in an actual Yb:YAG device structure.

Three sample structures were produced: Sample A had an uncoated YAG piece directly bonded to a polished tantalum substrate, Sample B had an uncoated YAG piece bonded to a CuW substrate, and Sample C had an HR-coated YAG substrate bonded to a CuW substrate with the HR coating at the bond line. Good bonds were obtained on all of the samples with only some delamination in the outer 2- to 3-mm edge of Sample C due to coating stress from the HR coating on the YAG substrate. A photo of Sample C is shown in Fig. 19. The delaminated area shows up as a faint ring near the edge.

The bonded samples were temperature cycled to over 150 °C. This resulted in some small voids forming in the bond line of the tantalum sample, but no changes to the CuW samples. The void formation is thought to be due to outgassing from the tantalum surface.

Due to the multiple optical surfaces (reflections) involved, it was difficult to get a good measurement of the surface figure of the bonded part with standard metrology equipment. Sample C measured below $\lambda/2$ over the central 0.5", while measurements on Samples A and B did not yield useful results. The YAG substrates had under $\lambda/10$ transmitted wavefront distortion and were thin enough to conform to the metal substrate surface. Most of the distortion originated from the edge roll during the polishing of the CuW substrates and can be improved with a better polishing process.

The authors are pleased to have demonstrated that it is possible to directly bond coated and uncoated YAG to CuW and tantalum metal substrates. More work remains to refine the process for optimum bond strength and to fully characterize thermal performance of the structure. It will also be interesting to investigate whether the bond strength is sufficient for additional postprocessing. Finally, performance of a directly bonded mount must be proven in an actual thin-disk laser structure, and compared to the other available mounting techniques detailed above.

6. Concluding Remarks

While the design of a typical thin-disk laser assembly does present challenges, it is the authors' hope that we have shed some light into the types of fabrication techniques available to enable their manufacture. Some of these techniques are quite standard in the optics industry and some are fairly novel; however, in the end, the ability to execute and consistently produce devices to specification is key. As laser designers continue to push power scaling and beam quality requirements of solid-state lasers to new levels, tolerances will tighten and new material systems and assembly configurations will be required. We look forward to continuing to contribute to these efforts.

7. Acknowledgments

Some of the work described above was funded by the Air Force Research Laboratory. The authors would like to especially thank Pete Latham, Tim Newell, and Vern Schlie (Integral Laser Solutions) for their continued support and insights.

References

[1]Scientific Materials Corporation, Yb:YAG product page, available at http://www.scientificmaterials.com/products/yb-yag.php.
[2]Rochford, K., "Polarization and polarimetry," in *Encyclopedia of Physical Science and Technology*, 3rd ed., vol. 12 (2001).
[3]Stewart, A. F., Lu, S., Tehrani, M., and Volk, C., Proc. SPIE **2114**, 662 (1994).
[4]Lyngnes, O., Traggis, N, and Li Dessau, K., Opt. Photonics News **17**(6), 28 (2006).
[5]Traggis, N., and Lyngnes, O., "Ion-beam sputtered high-laser-damage coatings on YAG for CW applications," in *SSDLTR 2009 Technical Digest*, Directed Energy Professional Society, p. 116 (2009).
[6]Lyngnes, O., "High laser damage coatings on YAG using ion beam sputtering deposition," in *SSDLTR 2009 Technical Digest*, Directed Energy Professional Society, p. Laser-6 (2006).
[7]Schlie, V., "Thin Disk Lasers (TDL) and Applications: CW, Pulsed, and USL," Directed Energy Symposium Short Course, Directed Energy Professional Society (2009).
[8]Myatt, C., Traggis, N., and Li Dessau, K., "Optical contacting grows more robust," Laser Focus World, p. 95, January (2006).
[9]Traggis, N., and Claussen, N., "Novel Technique for Producing Oversized Laser Gain Media in High Fluence Applications," in *SSDLTR 2009 Technical Digest*, Directed Energy Professional Society, p. 111 (2009).
[10]Traggis, N., and Claussen, N., SPIE Proc. **7578**, 75780F (2010).
[11]Traggis, N., and Claussen, N., "Epoxy Free Bonding for High Performance Lasers," 11th Annual Directed Energy Symposium Proceedings, Directed Energy Professional Society (2008).
[12]Smith, W.F., *Foundations of Materials Science and Engineering*, 3rd ed., McGraw-Hill (1993).
[13]Lobad, A., Stalnaker, D., Ross, S., Schlie, V., and Latham, W., "6.5kW, Yb:YAG Ceramic Thin Disk Laser," *SSDLTR 2009 Technical Digest*, Directed Energy Professional Society, p. 182 (2009).
[14]Giesen, A., and Speiser, J., IEEE J. Sel. Top. Quantum Electron. **13**(3), 598 (2007).
[15]Krupke, W.F., Shinn, M.D., Marion, J.E., Caird, J.A., and Stokowski, S.E., J. Opt. Soc. Am. B **3**(1), 102 (1986).

[16]*CRC Handbook of Chemistry and Physics*, 77th ed., CRC Press (1996).
[17]Epoxy Technology Inc., EPO-TEK® T7110 Technical Data Sheet, available at http://www.epotek.com/SSCDocs/datasheets/T7110.PDF.
[18]NuSil Technology LLC, CV-2946 Thermally Conductive, Controlled Volatility Silicone, Product Data Sheet, available at http://www.nusil.com/library/products/CV-2946P.pdf.
[19]Indium Corporation, Eutectic Gold/Tin Solder, available at http:www.indium.com/_dynamo/download.php?docid=328.
[20]Indium Corporation, Thermal Interface Materials, available at http://www.indium.com/TIM/solutions/liquidmetal.php.
[21]Tsunekane, M., Dascalu, T., and Taira, T., "High-power operation of diode edge-pumped, composite microchip Yb:YAG laser with ceramic pump wave-guide," Proceedings of Advanced Solid State Photonics 2005, paper TuB43 (2005).
[22]Potier, N., Sindzingre, T., and Rabia, S., "Fluxless Soldering Under Activated Atmosphere at Ambient Pressure," Proc. SMI, 453-458 (1995).
[23]Frear, D.R., Hosking, F.M., Keicher, D.M., and Peebles, H.C., "Fluxless Soldering for Microelectronic Applications," in *Materials for Electronic Packaging*, edited by D.D.L. Chung, Butterworth Heinemann, p. 79 (1995).
[24]Sasaki, J., Kaneyama, Y., Honmou, H., Itoh, M., and Uji, T., "Self-aligned Assembly Technology for Optical Devices Using AuSn Solder Bumps Flip-Chip Bonding," Proc. IEEE LEOS Annual Meeting, 260-261 (1992).
[25]Lee, S., and Chen, P., Development of High Performance Thermal Interface Material, Intel Technology Symposium, Seattle, WA, September 27–28 (2001).
[26]Webb, R., and Gwinn, J., Low Melting Point Thermal Interface Material, 2002 Inter Society Conference on Thermal Phenomena, pp. 671-676, 2002.
[27]Enerdyne Solutions, Products: Indigo, available at http://www.enerdynesolutions.com/prod_indigo.html.
[28]Lockheed Martin, Low Stress Optics Mount Using Thermally Conductive Liquid Metal or Gel, U.S. Patent No. 7551656 (2009).
[29]Liao, Y., Miller, R.J.D., and Armstrong, M.R., Opt. Lett. **19** 1343 (1999).
[30]Vetrovec, J., "Ultrahigh-Average Power Solid-State Laser," SPIE Proceedings, vol. 4760, High Power Laser Ablation Conference, April (2002).
[31]Chou, H.P., Sadovnik, I., Tammaro, E.J., and Wang Y.-L., "Thermo-Mechanical and Optical Analysis and Modeling for a Diamond-Cooled Solid State Nd:YAG Laser," SPIE Proceedings, vol. 6216, Laser Source and System Technology for Defense and Security II, 62160E-1 (2006).
[32]Millar, P., Birch, R.B., Kemp, A.J., and Burns, D.P., IEEE J. Quantum Electron. **44**(8), 709 (2008).
[33]Newburgh, G.A., Dubinskii, M., and Merkle, L.D., Electron. Lett. **43**, 5 (2007).
[34]Lindberg, H.,Strassner, M., Gerster, E., Bengtsson, J., and Larsson, A., IEEE J. Sel. Top. Quantum Electron. **11**(5), 1126 (2005).
[35]Kemp, A.J., Valentine, G.J., Hopkins, J.-M., Hastie, J.E., Smith, S.A., Calvez, S., Dawson, M.D., and Burns, D., IEEE J. Quantum Electron. **41**(2), 148 (2005).
[36]Van Loon, F., Kemp, A.J., MacLean, A., Calvez, S., Hopkins, J.-M., Hastie, J.E., Dawson, M.D., and Burns, D., Opt. Express **20**(14), 9250 (2006).
[37]Schepler, K.L., Peterson, R.D., Beny, P.A., and McKay, J.B., IEEE J. Sel. Top. Quantum Electron. **11**(3), 713 (2005).

The Authors

Nicholas G. Traggis is vice president at Precision Photonics Corporation. He has held various engineering and operations positions for the design, development, and commercial production of photonic and optical component products. Accomplishments include developing and bringing to production several, adhesive-free, optical contacting technologies widely utilized in high power solid-state laser construction, and leading the transition of several photonics products from prototype research stages into commercial production. Mr. Traggis holds a bachelor of science degree in materials engineering from the Colorado School of Mines.

Dr. Neil R. Claussen, a senior scientist at Precision Photonics Corporation, is focused primarily on epoxy-free bonding techniques for high power, solid-state lasers. Dr. Claussen has contributed to PPC's success in bonding complex, multilayer assemblies of dissimilar materials as well as making defect-free bonded apertures with areas exceeding 200 cm^2. He also heads up research and process development for new laser materials. Dr. Claussen completed his physics graduate work at the University of Colorado-Boulder.

Dr. Christopher S. Wood is the director of business development at Precision Photonics Corporation. Chris has experience with high power pulsed and CW lasers, laser-crystal mounting methods, laser efficiency and thermal analysis, and wavefront analysis from his previous work at Lockheed Martin Coherent Technologies. He has led challenging optical projects from R&D inception all the way through space qualification.

Dr. Ove Lyngnes is director of operations at Precision Photonics Corp. Dr. Lyngnes has over 15 years of experience working with optical coatings. Since he came to PPC in 2005, the coating technology at PPC has evolved into a world-class production and development facility specializing in ion beam sputtering deposition technology. Dr. Lyngnes graduated from the University of Arizona Physics Department in 1997 where he did his thesis work under the direction of Dr. Hyatt Gibbs.